Preparation and Characterization of EVA–Sisal Fiber Composites

M. E. Malunka, A. S. Luyt, H. Krump

Department of Chemistry, University of the Free State (Qwaqwa Campus), Phuthaditjhaba 9866, South Africa

Received 20 June 2005; accepted 19 September 2005
DOI 10.1002/app.23650
Published online in Wiley InterScience (www.interscience.wiley.com).

ABSTRACT: In this work, composites of an EVA polymer matrix and short sisal fiber were characterized. The physical-morphological as well as chemical interactions between EVA and sisal were investigated. When the samples were prepared in the presence of dicumyl peroxide, the results suggest that crosslinking of EVA as well as grafting between EVA and the sisal fibers took place. Morphological changes were studied by scanning electron microscopy (SEM). Results from Hg-porosimetry, SEM, Fourier transform infrared spectroscopy, surface free energy, and gel content strongly indicate grafting of EVA onto sisal under the composite preparation conditions, even in the absence of peroxide. The grafting mechanism could not be confirmed from solid-state ^{13}C NMR analysis. The grafting had an impact on the thermal and mechanical properties of the composites, as determined by differential scanning calorimetry and tensile testing. Thermogravimetric analysis results show that the composites are more stable than both EVA and sisal fiber alone. The composite stability, however, decreases with increasing fiber content. © 2006 Wiley Periodicals, Inc. J Appl Polym Sci 100: 1607–1617, 2006

Key words: composites; fibers; crosslinking; mechanical properties; thermal properties

INTRODUCTION

Recently, cellulosic fillers of fibrous nature have been of great interest, as they can yield composites with improved mechanical properties when compared with those containing non-fibrous fillers.[1] When used as reinforcing agents for composites, they offer a number of benefits when compared with mineral fillers, i.e., high specific stiffness and strength, desirable fiber aspect ratio, flexibility during processing with no harm to the equipment, low density, biodegradability and finally, low cost per unit volume basis. Several cellulosic products and wastes such as shell flour, wood flour, and pulp have been used as fillers in thermoplastics.[1,2] Additionally, the properties of cellulosic fibers compare favorably with other reinforcing fibers that are commonly used.[3] Natural fibers are much cheaper than synthetic fibers and could replace synthetics in many applications where cost savings outweigh strength requirements.[4] Sisal fiber is one of the most widely used natural fibers and is very easily cultivated. It has short renewal times and grows wild in the hedges of fields and railway tracks.[5] It is a hard fiber extracted from the leaves of the sisal plant (*Agave sisalana*).[6]

Mechanical performance of a fiber-reinforced plastic composite primarily depends on three factors: (a) strength and modulus of the fiber, (b) strength and chemical stability of the resin, and (c) effectiveness of the bond between resin and fiber in transferring stress across the interface.[7] Many of the properties of fibrous composite materials are strongly dependent on microstructural parameters such as fiber diameter, fiber length, volume fraction of fibers, and alignment and packing arrangement of fibers. In randomly oriented short fiber composites, the fiber length and content play an important role in determining their mechanical performance.[2] The dynamic mechanical properties of short sisal fiber-reinforced polypropylene composites containing both untreated and treated fibers have been studied with reference to fiber loading, fiber length, chemical treatments, frequency, and temperature.[8] The incorporation of short sisal fiber into polypropylene caused the storage moduli (E') and loss moduli (E'') to increase, but the mechanical loss factor ($\tan \delta$) to decrease. The storage modulus decreased with increase in temperature. The treated fiber composites show better properties when compared with untreated system.

Satyanarayana and co-workers[9] studied the effects of fiber diameter, test length, and test speed on the tensile strength, initial modulus, and percent elongation at break of sisal fibers. They found no significant variation of mechanical properties with change in fi-

Correspondence to: A. S. Luyt (luytas@qwa.uovs.ac.za).
Contract grant sponsor: The South African National Research Foundation; contract grant number: GUN 2050677; Contract grant sponsor: University of the Free State.

ber diameter, but the tensile strength and percent elongation at break decreased and Young's modulus increased with fiber length. Yang et al.[10] studied the effect of thermal treatment on the chemical structure and crystallinity of sisal fiber. They found that the chemical structure of sisal fibers will not change below 200°C, while the degree of crystallinity will increase.

Several types of polymers were used as matrices for natural fiber composites.[2] The most commonly used are thermoset polymers such as polyester, epoxies, and phenolics. Thermoplastics like polyethylene, polystyrene, and polypropylene were also recently used as matrices. These polymers may have different affinity towards the fiber because of the differences in their chemical structure. As a consequence, the reinforcement effect of the fibers in these matrices may vary widely. Very few studies have been reported in literature on the use of sisal fiber as reinforcement in thermoplastic polymers like low-density polyethylene (LDPE) and thermosetting polymers like epoxy and phenol–formaldehyde.

The problem encountered when attempting to combine plant fibers or ligno-cellulosic material with a thermoplastic or thermoset matrix is one of incompatibility. Several investigators[11,12] studied the surface morphology, as well as mechanical and degradation properties, of surface treated fibers. Yang et al.[11] studied the relationship between surface modification and tensile properties of sisal fibers. Their modification methods included alkali, H_2SO_4, conjoint H_2SO_4 and alkali, benzol/alcohol de-wax, acetylated, thermal, alkali- thermal, and thermal-alkali treatments.

The mechanical properties of sisal fiber composites (randomly oriented) of several thermoset resin matrices (polyester, epoxy, phenol–formaldehyde) and a thermoplastic matrix (LDPE) were evaluated with respect to fiber length and fiber loading.[2] All the composites showed a general trend of increase in properties with fiber loading. However, the optimum length of the fiber, required to obtain an increase in properties, varied with the type of matrix. A study of the mechanical behavior of high-density polyethylene, reinforced with continuous henequen fibers (*Agave fourcroydes*), showed that fiber–matrix adhesion was promoted by fiber surface modifications using an alkaline treatment and a matrix preimpregnation together with a silane coupling agent.[13] Joseph et al.[14] investigated the mechanical, rheological, electrical, and viscoelastic properties of short sisal fiber-reinforced LDPE composites as a function of processing method, fiber content, and fiber length and orientation. They found that longitudinally oriented composites showed maximum storage moduli, and that a critical fiber length of 6 mm was necessary to obtain maximum dynamic moduli. They also compared the experimentally observed tensile properties of short sisal fiber-reinforced LDPE composites with the existing theories of reinforcement.[15] They found that the tensile properties of short fiber-reinforced composites strongly depend on fiber length, fiber loading, fiber dispersion, fiber orientation, and fiber matrix interfacial bond strength.

The influence of sisal fiber content and different concentrations of dicumyl peroxide (DCP) on the thermal, mechanical, and viscoelastic properties of short sisal fiber-linear low-density polyethylene (LLDPE) composites was investigated.[16] Addition of low concentrations (1%) of curing agent (DCP) to the composites prepared by mechanical mixing and subsequent melt pressing of LLDPE and milled sisal fibers significantly improved their tensile and viscoelastic properties. However, a high DCP concentration (3%) also induced degradation of the matrix at low sisal contents. The effect of peroxides (DCP and dibenzoyl peroxide) treatment on the tensile properties of sisal fiber-reinforced LDPE composites at 30% fiber loading was investigated.[12] The tensile values of the composites increased with an increase in concentration of peroxide up to a certain level (4% for DCP and 6% for BP) and then remained constant. From the scanning electron microscopy (SEM) photomicrographs of the tensile fracture surfaces of DCP- and BP-treated sisal fiber–LDPE composites, it was found that PE was grafted onto the cellulose surface. A similar type of peroxide induced PE grafting onto cellulose fiber was reported by Sapieha et al.[17]

Hybrid composites prepared by the incorporation of two or more different types of fibers into a single polymer matrix also received attention. The influence of the relative composition of short sisal/glass fibers, their length, and distribution on the tensile properties of short sisal/glass intimately mixed polyethylene composites was examined.[18] Chemical surface modifications such as alkali, acetic anhydride, stearic acid, permanganate, maleic anhydride, silane, and peroxides given to the fibers and matrix were found to be successful in improving the interfacial adhesion and compatibility between the fiber and matrix. Among the various chemical modifications, the best tensile strength and modulus was exhibited by the SGRP with benzoyl peroxide-treated fibers. This is attributed to the peroxide-initiated grafting of polyethylene on to the fibers.

EXPERIMENTAL

Materials

In this work, EVA 750 with 9% vinyl acetate (VA) content ($\rho = 0.930$ g cm^{-3}, $T_m = 95$°C, tensile strength of 19 MPa, and 750% elongation at break) was supplied by Plastamid, Elsies River, South Africa. DCP ($T_m = 39–41$°C, decomposition at temperatures above 88°C), supplied by Sigma–Aldrich, Johannesburg,

South Africa, was used as crosslinking agent. Sisal (*Agave sisalana*) fiber was obtained from the National Sisal Marketing Company in Pietermaritzburg, South Africa.

Preparation of composites

The long fibers were cut into small pieces with lengths between 5 and 10 mm. This fiber was washed with petroleum ether by soaking at 40°C for 5 h (regular shaking was necessary). It was then washed thoroughly with warm distilled water and dried at 80°C overnight. Samples of EVA, sisal fiber, and DCP (where crosslinking was required) were mechanically melt-mixed at different ratios in a Brabender Plastograph. A mixing temperature of 120°C and a mixing speed of 30 min^{-1} were used. The 35 g samples were mixed for 10 min. and melt-pressed at 120°C and 100 bar for 5 min.

Extraction

The gel content was determined through toluene extraction of the uncrosslinked part of the samples. Samples were wrapped in fine stainless steel mesh and tied with a string, placed in a round-bottomed flask half-filled with toluene, and refluxed for 12 h. After extraction, the wrapped samples were washed with chloroform and first dried at room temperature for 24 h, followed by 50°C drying in an oven for 24 h, to evaporate all the chloroform. The samples were reweighed and the gel content was determined by calculating the percentage ratio of the mass of toluene-insoluble gel to that of the sample before extraction, using eq. (1).

$$\% \text{ Gel} = xM_1 - M_2 - M_3/xM_1 \quad (1)$$

where M_1 is the mass of the sample, M_2 the mass of the sample + mesh + wire (before extraction), M_3 the mass of the sample + mesh + wire (after extraction), and x is the fraction of the sample which excludes sisal. Sisal was excluded in the calculations because it does not dissolve in toluene.

Thermomechanical analysis

Thermomechanical analyses (TMA) were carried out at expansion mode in a Perkin–Elmer TMA 7 thermomechanical analyser under flowing nitrogen atmosphere. Polymer samples (height 5 mm) were heated from 30 to 75°C at 5°C min^{-1}, then cooled to 30°C, and heated again under a force of 10 mN.

Characterization of EVA–sisal morphology

The morphological aspects of the EVA–sisal interfaces at fracture surfaces were observed by using a Jeol 6400 WINSEM SEM model at 5 keV.

Pore size determination

A mercury porosimetry method was used for the determination of the total volume between the EVA monofilaments and the pore volumes in the EVA composite with treated and untreated fibers, the evaluation of pore size distributions, as well as the determination of the specific surface. The measurements were carried out in a Porozimetro 1500 Carlo Erba instrument connected to a calculation unit CVT 960. The maximum used pressure of mercury was 150 MPa, which allowed determination of pore sizes down to 5 nm.

Fourier transform infrared spectroscopy

Analyses were done in a Shimadzu Fourier transform infrared spectroscopy (FTIR) 8700 spectrometer with a combination of a highly sensitive MCT detector connected to an infrared microscope AIM 8800. Spectra were recorded from 720 to 4000 cm^{-1} with a 4 cm^{-1} resolution. An ATR objective with a germanium crystal (magnification 15×) was used. The detected measured area was 100 × 100 μm.

Differential scanning calorimetry

Differential scanning calorimetry (DSC) analyses were carried out in a Perkin–Elmer DSC 7 thermal analyser under flowing nitrogen atmosphere. The instrument was calibrated using the onset temperatures of melting of indium and zinc standards, and the melting enthalpy of indium. Polymer samples (between 5 and 10 mg) were initially heated from 25 to 150°C at 10°C min^{-1}, held at that temperature for 1 min to eliminate thermal history effects, and then cooled to 25°C at 10°C min^{-1}. They were kept there for 1 min, heated again to 150°C at 10°C min^{-1}, and cooled to 25°C at the same rate. Onset and peak temperatures of melting and crystallization, as well as melting and crystallization enthalpies, were determined from the second scan where ΔH_m is the melting enthalpy of the samples calculated from the main melting peak.

Thermogravimetric analysis

Thermogravimetric analyses (TGA) were carried out in a Perkin–Elmer TGA 7 thermogravimetric analyzer. Polymer samples (between 5 and 10 mg) were heated from 25 to 600°C at 20°C min^{-1} under flowing nitrogen.

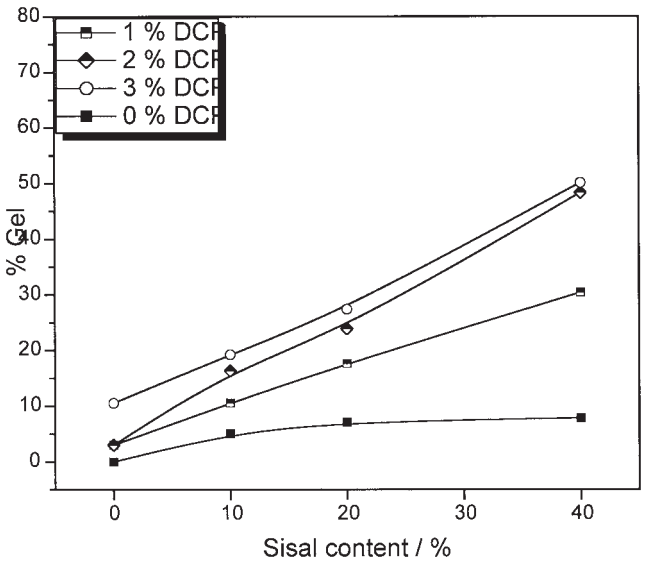

Figure 1 Gel content of EVA–sisal composites.

Tensile testing

The mechanical properties were determined using a Hounsfield H5KS tensile tester at a cross-head speed of 50 mm min^{-1}. Dumbbell-shaped specimens with a thickness of 1.3 mm, average width of 4.9 mm, and gauge length of ~24 mm were used. In total, five dumbbells per composite sample were used for each analysis and the average was taken as the reported value.

Surface free energy evaluation

For the determination of the total surface free energy, as well as its disperse and polar parts, of the samples, a surface energy evaluation system (SEES, Czech Republic) was used. The SEES software is able to determine the polar and disperse components of the total surface free energy with standard deviation. In this work, contact angle measurements[8] were done by the drop method using the Owens-Wendt regression method

$$(1 + \cos\theta_i)\gamma_{li} = 2(\sqrt{\gamma_s^d \gamma_{li}^d} + \sqrt{\gamma_s^p \gamma_{li}^p}) \qquad (2)$$

where i indicates the used liquid. The sum of the disperse γ_s^d and polar γ_s^p components gives the value of the total surface free energy. Five liquids of different polarity were used (water, aniline, formamide, benzyl alcohol, and ethylene glycol). For each measurement, 15 drops of each of the liquids were used to ensure reproducibility at the laboratory temperature.

^{13}C nuclear magnetic resonance spectroscopy

Solid-state ^{13}C NMR spectra were measured on a Bruker Avance 500 spectrometer at a frequency of 125.8 MHz under conditions that allow quantitative analysis (spinning frequency 10 kHz, contact time 2 ms).

RESULTS AND DISCUSSION

The dependence of the gel content on the DCP content in the composites for various sisal concentrations is shown in Figure 1. The gel content of the pure EVA matrix increases only slightly with increasing DCP content. This suggests that EVA crosslinks only slightly under the conditions used, which is to be expected, since the half-life of decomposition of DCP is much longer than the processing time at the temperature at which the samples were prepared. This was done on purpose, because we did not want crosslinking effects to overshadow grafting effects. It is also important to note that sisal fiber was excluded in the gel content calculations,

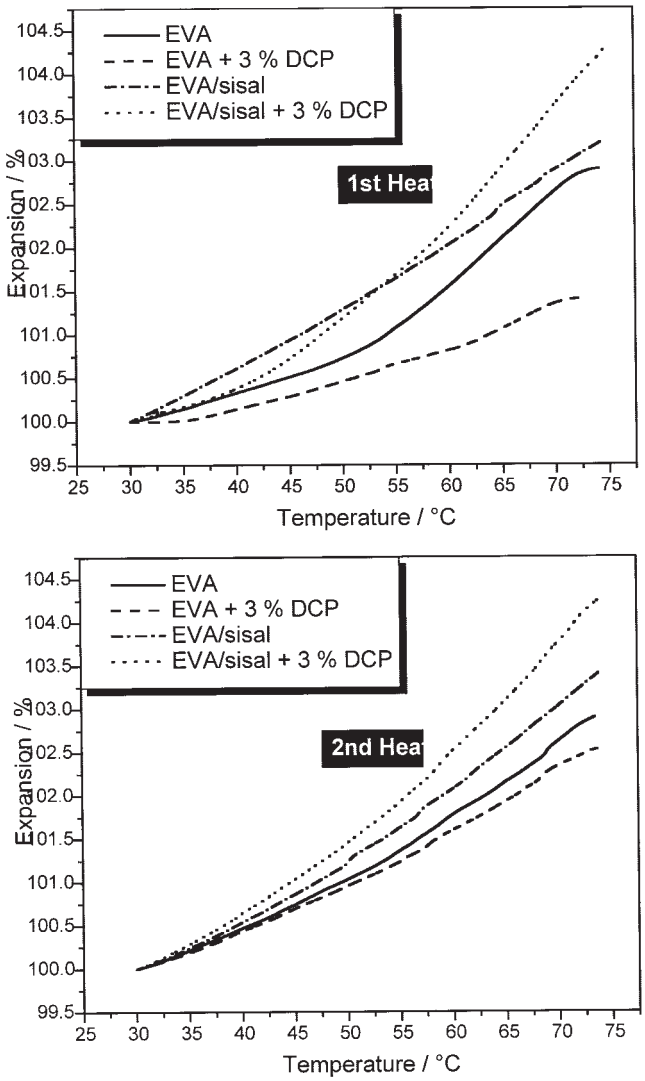

Figure 2 TMA analyses of EVA and its composites.

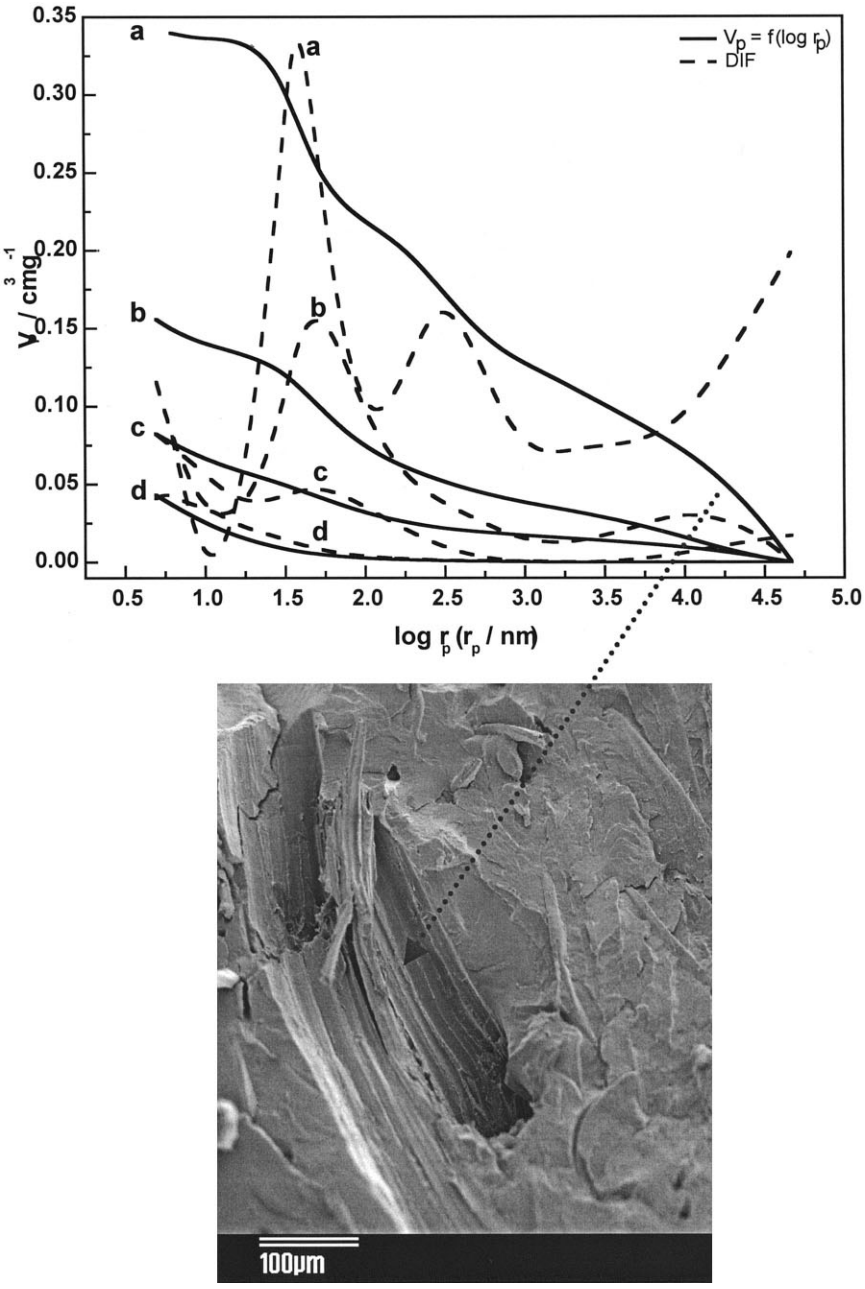

Figure 3 Hg-porosimetry of (a) sisal fiber, (b) EVA–sisal composite, (c) EVA–sisal composite prepared in the presence of DCP, and (d) EVA, linked to an SEM micrograph of an EVA–sisal composite.

because it does not dissolve in toluene. It is therefore interesting that an increase in gel content was observed with an increase in sisal fiber content, even when no DCP was mixed into the composite. This suggests that thermomechanical friction during the mixing in the Brabender causes slight grafting between the sisal fiber and the EVA matrix, even in the absence of peroxide. In the presence of DCP, the gel content increases substantially with increasing sisal fiber content. A possible explanation could be that the higher sisal fiber content caused higher friction during the mixing in the Brabender. This could cause an increase in temperature, which could lead to more efficient crosslinking of the EVA. However, as mentioned before, slight grafting was observed in the absence of DCP, so that the crosslinking of the EVA was probably also accompanied by grafting between the EVA and sisal fiber. However, the difference in temperature between the mixing of samples containing 10 and 40 wt % of sisal fiber was only 2–3°C. This small temperature difference could not have such a big influence on the creation of a higher crosslink density as is shown in Figure 1. This suggests that grafting between sisal fiber and

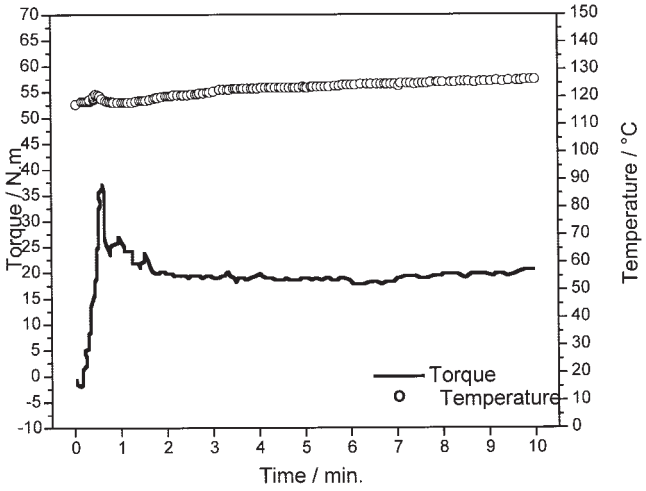

Figure 4 Torque and temperature scans during blending in the Brabender mixer.

the EVA matrix in the presence of DCP most probably took place.

Confirmation of crosslinking or grafting can be obtained through TMA analysis, which is a highly sensitive method for the measurement of crosslinked or filled materials, such as composites. For this reason, a pure EVA matrix, an EVA matrix prepared in the presence of DCP (3%), an EVA matrix with 20% sisal fiber, and an EVA matrix with 20% sisal prepared in the presence of DCP (3%) were investigated by TMA. From Figure 2 (first heating) it is clear that the pure EVA matrix has a higher volume expansion than the EVA matrix prepared in the presence of DCP. This

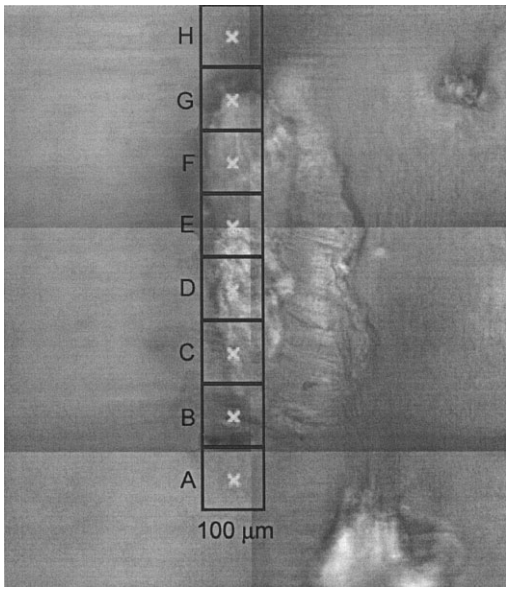

Figure 5 Cross section of an EVA–sisal composite, prepared in the presence of DCP, on which FTIR analyses were done.

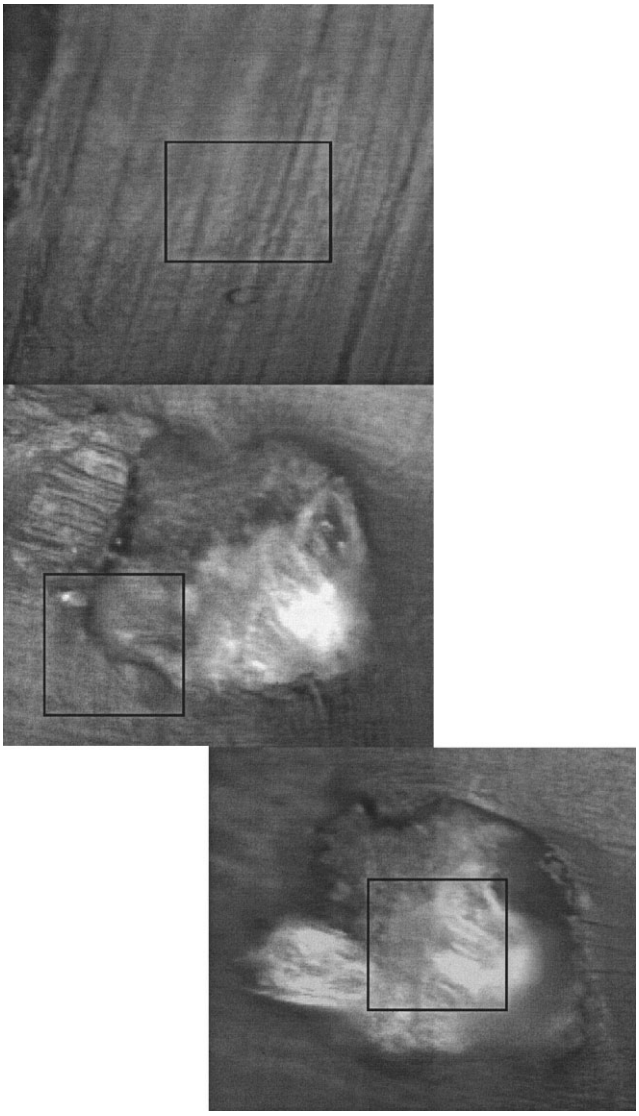

Figure 6 Cross section of the EVA matrix (above), interface (middle), and sisal fiber (bottom) indicating positions where FTIR spectra were taken.

confirms crosslinking, because the crosslinked chains do not have so much space for movement when compared with the uncrosslinked chains. In the presence of sisal fiber, an increase in volume expansion was observed. This is even more pronounced for the sample prepared in the presence of DCP. Because the T_g of cellulose is around 240°C (that of EVA is around −25°C),[12] we can ignore the motion of the cellulose chains, because the temperature scale during the measurement was between 30 and 75°C. The only explanation is the presence of a water residue in the pores of the sisal fiber. Despite the drying of sisal fibers before blending in the Brabender, sisal fibers are very hydrophilic (see Fig. 12). During the heating, there probably was evaporation of water that led to the expansion of the sample. The expansion is even greater for the sample prepared in the presence of

DCP, probably because the crosslink network traps the water in the sisal structure. Figure 2 also shows the effect of residual thermal stresses on the TMA measurement. During the first heating, the TMA expansion results show the occurrence of an undulation. This reflects the release of stress. When the sample is cooled and then reheated, the material is free of thermal stresses or other thermal history.

In spite of the fact that sisal fiber looks like a monofilament, it is clear from the Hg-porosimetry of sisal fibers (solid line, Fig. 3) and from the SEM micrograph that sisal fiber is not a monofilament, but a multifilament. Another confirmation of this is the size of pores being higher than 20 μm ($>\log r_p = 4$). We can assume that these pores come from the inter-filament areas. The volume ratio of these pores is ~20%. From the Hg-porosimetry of sisal fibers, it is also evident that there are two different types of pores. The first peak appears at a log r_p of ~2.5, which is equivalent to a pore diameter of 700 nm. The volume of these pores is 0.165 $cm^3\ g^{-1}$. The second peak appears at approximately log $r_p = 1.60$, which is equivalent to 80 nm. The volume of these pores is 0.28 $cm^3\ g^{-1}$. From this, it is evident that the very small pores of ~80 nm make up the largest part of the pore volume in the sisal fiber. In the EVA–sisal fiber sample, the volume ratio of the pores with log r_p higher than 4 decreased from 20 to 9%. There is also a substantial decrease in the sizes of the other two peaks (in the case of log $r_p = 2.5$ the decrease is from 0.165 to 0.05 $cm^3\ g^{-1}$, and in the case of log $r_p = 1.60$, the decrease is from 0.28 to 0.11 $cm^3\ g^{-1}$). This indicates that EVA fills the pores in the sisal fiber, the extent of which will depend on the viscosity of the blend during the mixing in the Brabender. This effect is even more pronounced for the sample prepared in the presence of 3% DCP. Compared to the EVA–sisal fiber composite, the volume of the pores with log r_p higher than 4 and log $r_p = 2.5$ decreased almost to the same level as that of the pure EVA matrix. In the case of log $r_p = 1.60$, the decrease is from 0.28 $cm^3\ g^{-1}$ (for the sisal fiber) to 0.11 $cm^3\ g^{-1}$ (for the EVA–sisal composite) to 0.04 $cm^3\ g^{-1}$ for the composite prepared in the presence of 3% DCP. This substantial decrease in the pore volume, especially when the sample is prepared in the presence of DCP, can be explained as follows: GPC analysis did show a slight increase in molecular weight of the EVA matrix treated with 3% DCP, indicating a low level of crosslinking, which is in line with the gel content results (Fig. 1). However, the increase in temperature from 117 to 125°C (Fig. 4) during the mixing of EVA and sisal in the presence of DCP indicates that not only crosslinking of EVA itself but also grafting between EVA and sisal took place. This explains the decrease in pore volume observed for the composite sample prepared in the presence of DCP. Because of chemical bonding between EVA and sisal, the molecules of Hg cannot easily fill the pores in the sisal structure.

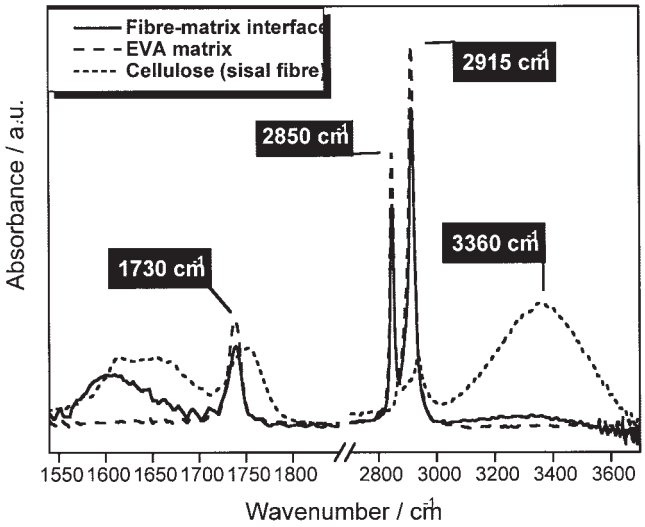

Figure 7 FTIR spectra of the EVA matrix, sisal fiber, and the sisal fiber–EVA matrix interface.

For confirmation of grafting, infrared spectra were obtained. The highly magnified cross section of EVA–sisal fiber (prepared in the presence of 3 wt % DCP) was analyzed by FTIR. As Figure 5 shows, eight different areas were scanned by the FTIR. For a more thorough investigation of the EVA–sisal fiber interface, spectra were obtained for the interface, pure EVA, and pure sisal fiber (Fig. 6). The spectra obtained from the cross-sectional areas are shown in Figure 7. The spectrum of the pure EVA matrix consists of strong C—H vibrations in the 2850 and 2920 cm^{-1} region. The peak belonging to the acetyl group (vibration of the C═O ester of the carboxyl group) appears at 1730 cm^{-1}. In the case of sisal fiber, a huge broad peak appears at 3360 cm^{-1} that belongs to the OH group. Grafting between EVA and sisal should give rise to a decrease in the 1730 and 3360 cm^{-1} peak intensities, because grafting will most probably involve reaction between C═O and OH groups. The spectrum for the fiber–matrix interface in Figure 7 clearly shows a decrease in the intensities of these peaks.

It has been assumed, and indications are, that grafting links are formed between —C═O on the vinyl acetate and —OH on the cellulose. It is, however, important to resolve the actual grafting mechanism in this system. We therefore obtained ^{13}C NMR spectra of the pure EVA and DCP-treated EVA and EVA–sisal samples (Fig. 8). The spectrum of EVA shows strong peaks at 33 and 31 ppm that correspond to the ethylene carbons in the crystalline and amorphous regions of EVA, respectively. Weak signals at 168.5 ppm (C═O), 73 ppm (CH), 38 ppm (CH_2), and 21 ppm (CH_3) correspond to the VA carbons. Weak signals at

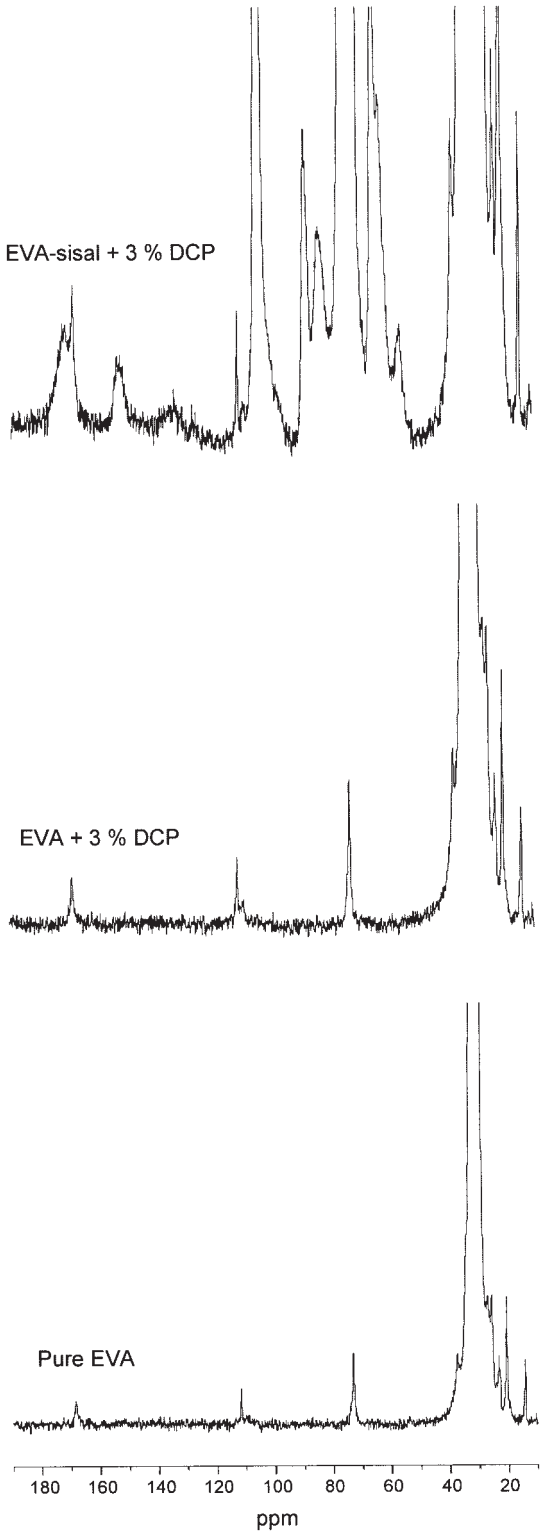

Figure 8 ^{13}C NMR spectra of (a) pure EVA, (b) 3% DCP-treated EVA, and (c) 3% DCP-treated EVA–sisal.

15, 24, and 27 ppm correspond to signals from polyethylene branches. Comparison of the integrated signal intensities shows that the EVA contains 2.3 mol % VA units, compared with the 2.9% corresponding to the 9% according to product specifications. The spectrum of DCP-treated EVA is exactly the same as that of pure EVA. This is to be expected, because the extent of crosslinking was very low for this sample, probably below the detection limit of the NMR spectrometer. The DCP-treated EVA–sisal composite shows, in addition to the peaks described above, signals at 106 ppm (C1), 72–76 ppm (C2, C3, and C5), 89 and 84 ppm (C4 in crystalline and amorphous regions), 66 and 63 ppm (C6 in crystalline and amorphous regions), as well as 171.5 ppm (C═O in sisal). Integrated line intensities show a slight decrease in polyethylene segment crystallinity: pure EVA (57.0%) > 3% DCP-treated EVA (56.0%) > 3% DCP-treated EVA–sisal composite (54.9%). This is in line with the DSC results discussed later. The NMR spectrum also does not show any graft points in this case, which means that the extent of grafting is below the detection limit of the spectrometer. This is possible because the total gel content for this sample is only about 25%, and grafting may occur along different routes.

DSC curves of EVA with different DCP contents are shown in Figure 9. It is evident that an increase in DCP content causes a decrease in the melting enthalpy of EVA. As was mentioned before, crosslinking of EVA initiated by DCP causes lower mobility of the chains, giving rise to lower crystallinity. When EVA–sisal composites, prepared in the absence of DCP, were analyzed, the peak size decreased because of the reduced amount of EVA in the samples, and the peaks shifted to lower temperatures with increasing amount of sisal in the samples (Fig. 10). For all the EVA–sisal fiber samples, prepared in the absence of DCP, the expected enthalpies are higher than the measured enthalpies (Table I). This is because the mobility of the

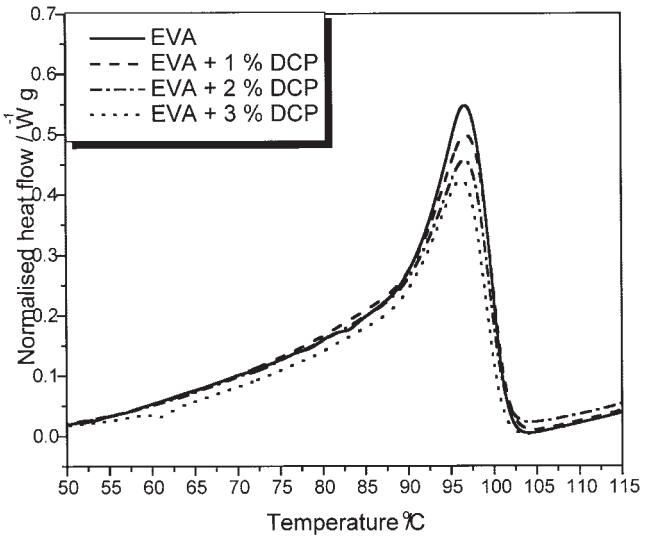

Figure 9 DSC heating curves of EVA with different DCP contents.

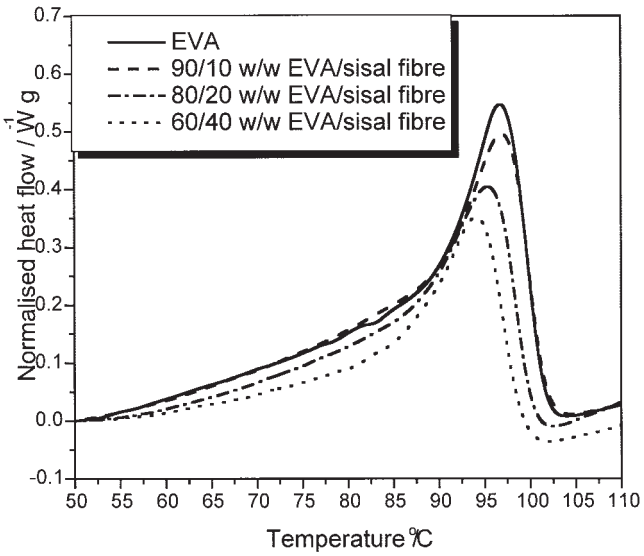

Figure 10 DSC heating curves of EVA with different sisal fiber contents.

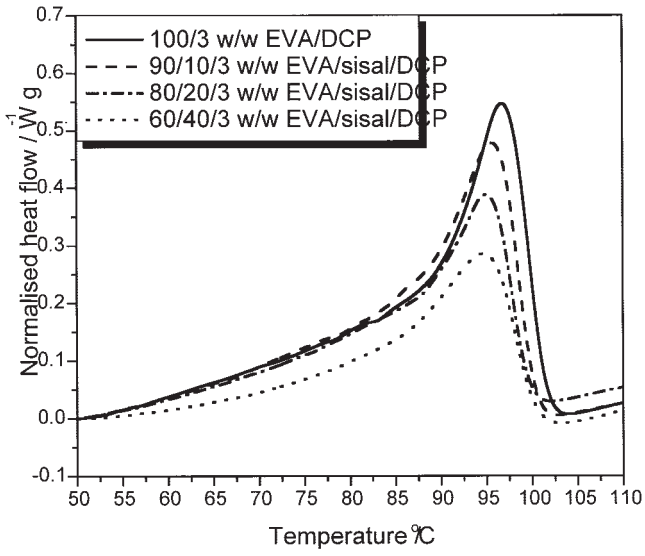

Figure 11 DSC heating curves of EVA with 3% DCP and different sisal fiber contents.

EVA chains decreases as a result of grafting.[13] This then leads to the formation of thinner crystal lamellae (confirmed by the shifting of the peaks towards a lower temperature) and lower crystallinity. This can also be seen in Figure 11 for EVA–sisal fiber samples prepared in the presence of DCP.

Figure 12 shows the TGA curves for EVA, sisal fiber, and the composites. The thermal decomposition of each sample takes place in the programmed temperature range of 50–600°C. In the case of sisal fiber, the weight loss between 60 and 100°C corresponds to the vaporization of water in the sample. The second weight loss at about 325°C is due to the thermal depolymerization of hemicellulose and the cleavage of the glucosidic linkages of cellulose. In the case of EVA, two decomposition steps are observed. The first step involves the degradation of VA groups, and the second one the degradation of the main chain. The results show that the fiber degrades before the EVA matrix, and that the composites are more stable than both EVA and sisal fiber alone. The composite stability does not depend on the amount of sisal, because in all cases the sisal decomposes first, followed by the decomposition of EVA.

Grafting and crosslinking have a substantial impact on the mechanical properties. The stress at break for EVA (in the absence of sisal) decreases with increasing

TABLE I
Summary of DSC Data for Crosslinked and Uncrosslinked EVA–Sisal Composites

EVA/sisal/DCP (w/w)	$T_{p,m}$ (°C)	$T_{o,m}$ (°C)	ΔH_m (J g^{-1})	Expected ΔH_m (J g^{-1})
100/0/00	97.4	87.3	56.7	
90/10/00	97.1	86.2	41.6	51.1
80/20/00	95.0	86.5	36.2	45.4
60/40/00	94.4	84.7	27.2	34.1
100/0/01	96.7	89.5	42.3	
90/10/01	96.6	87.1	39.1	38.1
80/20/01	96.5	86.2	36.3	33.8
60/40/01	93.9	81.9	24.4	25.4
100/0/02	97.2	87.9	41.8	
90/10/02	96.3	86.9	38.1	38.2
80/20/02	95.4	86.6	33.5	33.8
60/40/02	95.4	82.1	23.3	24.7
100/0/03	97.0	84.8	37.2	
90/10/03	96.1	84.4	33.1	33.5
80/20/03	95.2	84.4	27.6	29.8
60/40/03	94.5	81.4	20.8	22.3

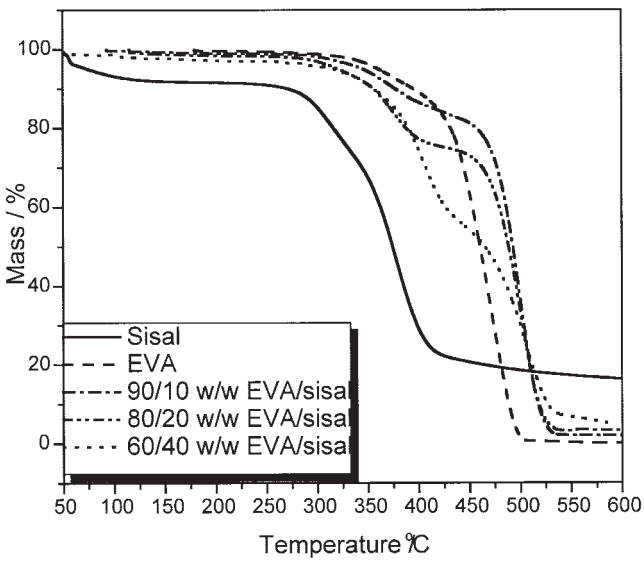

Figure 12 TGA curves of sisal fiber, EVA matrix, and EVA–sisal fiber composites.

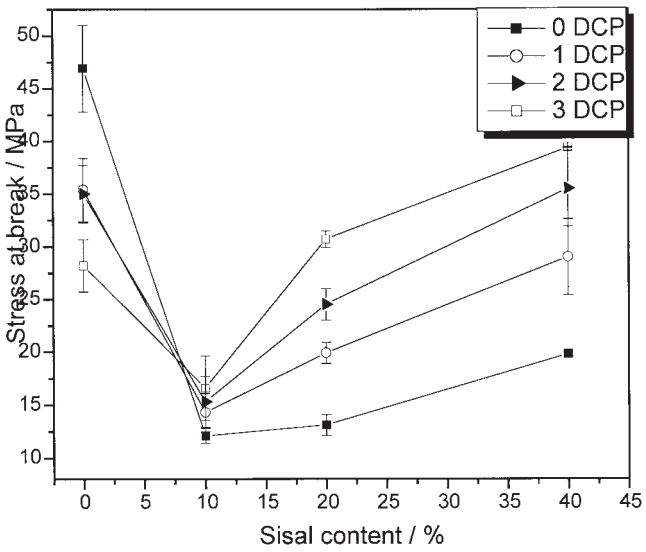

Figure 13 Effect of sisal fiber and DCP contents on the stress at break of the composites.

DCP content (Fig. 13). Since crosslinking reduces crystallinity, this observation is expected. The presence of 10 wt % sisal considerably reduces the stress at break of EVA, even for samples prepared in the presence of DCP. The reason is probably the weak interaction between EVA and sisal, and since it does not seem as if there is substantial grafting at this fiber loading (Fig. 1), a decrease in ultimate strength should be expected. Increased sisal contents give rise to increased stress at break values, especially for the samples prepared in the presence of increased amounts of DCP. Since it has been established that there is a strong element of grafting between EVA and sisal fiber (see discussion earlier), there will be stronger interaction between EVA and sisal fiber, which should give rise to increasing stress at break values. Crosslinking and grafting restrain chain movement, giving rise to decreasing elongation at break (Fig. 14). Increasing sisal content as well as crosslinking and grafting give rise to higher values of Young's modulus (Table II).

TABLE II
Modulus of Uncrosslinked and Crosslinked EVA/Sisal Composites

EVA/Sisal/DCP (w/w)	E ± SE (MPa)
100/0/00	120.8 ± 52.5
100/0/01	109.1 ± 9.0
100/0/02	99.3 ± 6.2
100/0/03	69.3 ± 9.2
90/10/00	239.0 ± 17.9
90/10/01	228.5 ± 31.2
90/10/02	216.0 ± 46.2
90/10/03	179.5 ± 9.5
80/20/00	352.2 ± 24.1
80/20/01	420.3 ± 32.6
80/20/02	428.6 ± 29.8
80/20/03	435.9 ± 86.0
60/40/00	523.3 ± 36.1
60/40/01	273.0 ± 13.0
60/40/02	582.2 ± 13.4
60/40/03	553.2 ± 21.2

Crosslinking and grafting should have an impact on the surface free energy. Figure 15 shows that the pure EVA matrix has a partially polar character, which is evident from the value of the polar component of the surface free energy. There is a decrease in the value of the polar component and an increase in that of the nonpolar component for DCP-treated EVA. This must be the result of crosslinking, which will give rise to a

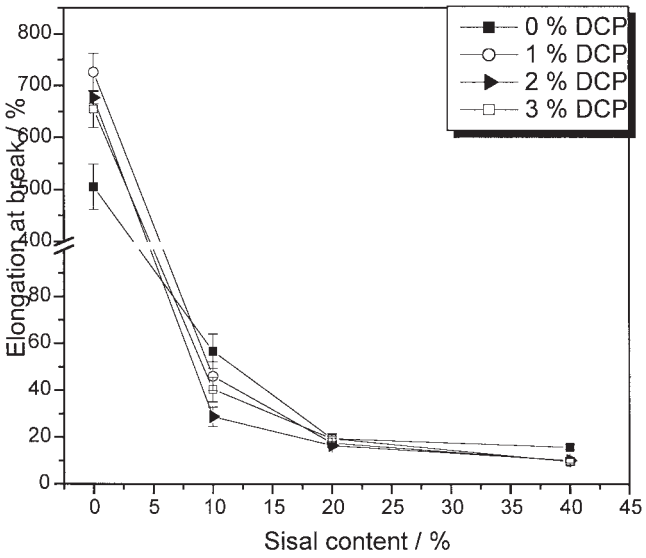

Figure 14 Effect of sisal fiber and DCP contents on the elongation at break of the composites.

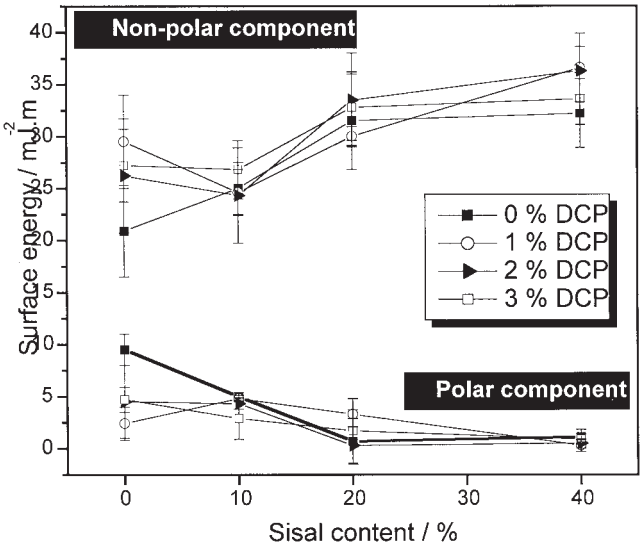

Figure 15 Nonpolar and polar components of the surface free energy of the composites.

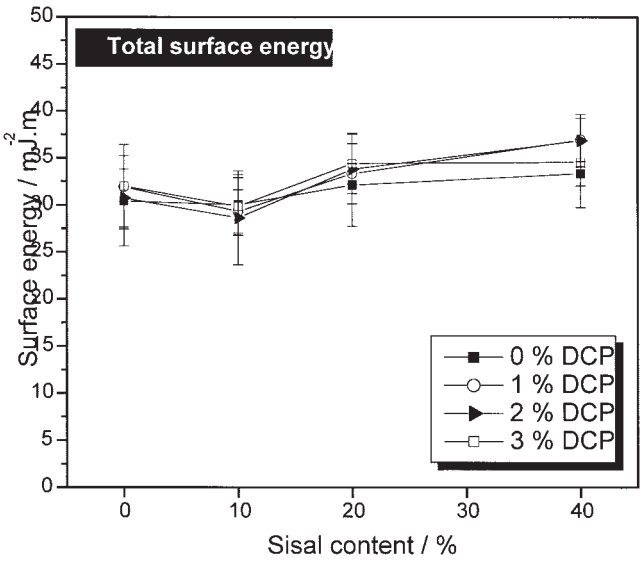

Figure 16 Total surface free energy of the composites.

reduction in the number of polar VA groups. The same trend is observed for EVA–sisal composites prepared in the absence of DCP, where there is a decrease in the value of the polar component and an increase in that of the nonpolar component with increasing sisal content. Sisal fiber consists of cellulose (strong polar character), and therefore an increase in sisal content should increase the value of the polar part of the surface free energy of the composites if there is no interaction between EVA and sisal fiber. As was mentioned before, grafting probably takes place through the OH groups in cellulose and the acetate groups in EVA, even in the absence of DCP, reducing the number of polar groups in the samples. The decrease of the value of the polar component and an increase in that of the nonpolar component become more evident with an increase in sisal fiber content. A slight increase in the total surface free energy with an increase in sisal fiber content was also observed (Fig. 16).

CONCLUSIONS

In this work, we presented and discussed the preparation and characterization of EVA–sisal fiber composites. All the results strongly point to grafting between EVA and sisal, even for samples prepared in the absence of DCP. Gel content results show slight crosslinking of DCP-treated EVA. There is, however, a strong increase in gel content for samples containing sisal fiber, indicating grafting between EVA and sisal fiber. Grafting between EVA and sisal has been confirmed by porosity measurements, FTIR analyses, and surface free energy measurements. The grafting mechanism could, however, not be established through solid-state ^{13}C NMR analysis.

The incorporation of sisal in the EVA matrix increases the composites' stiffness. The influence of DCP on the stiffness, however, depends on the amount of sisal in the composite. For 0 and 10% sisal, the tensile modulus decreases with increasing DCP content. For 20 and 30% sisal, the tensile modulus increases with increasing DCP content, probably because of grafting between EVA and sisal. Elongation at break increases in the presence of DCP, but drastically decreases in the presence of sisal. For pure EVA, stress at break decreases with increasing DCP content, probably because of degradation. It also decreases when 10% sisal is present in the EVA matrix, but increases for higher sisal contents. In the presence of sisal, increasing DCP content also increases stress at break, probably because of grafting between EVA and sisal.

Crosslinking and grafting also had an impact on the surface free energy of the samples. Generally, the values of the polar component decreased with increasing sisal and DCP contents.

Dr. Vladimir Khandl is acknowledged for doing the Hg-porosimetry measurements on the samples.

References

1. Amash, A.; Zugenmaier, P. J Appl Polym Sci 1997, 63, 1143.
2. Joseph, K.; Varghese, S.; Kalaprasad, G.; Thomas, S.; Prasannakumari, L.; Koshy, P.; Pavithran, C. Eur Polym Mater 1996, 32, 1243.
3. Joseph, K.; Thomas, S.; Pavithran, C. Comp Sci Technol 1995, 53, 99.
4. Maiti, S. N.; Singh, K. J Appl Polym Sci 1998, 32, 4285.
5. Albano, C.; Gonzalez, J.; Ichazo, M.; Kaizer, D. Polym Degrad Stabil 1999, 66, 179.
6. Berlin, A. A.; Volfson, S. A.; Enikolopian, N. S.; Negmator, S. S. In Principles of Polymer Composites; Henrici-Olive, G., Olive, S., Eds.; Springer-Verlag: Berlin, 1986.
7. Li, Y.; Mai, Y.-W.; Ye, L. Comp Sci Technol 2000, 60, 2037.
8. Joseph, P. V.; Mathew, G.; Joseph, K.; Groeninckx, G.; Thomas, S. Compos Part A: Appl Sci Manufact 2003, 34, 275.
9. Chand, N.; Satyanarayana, K. G.; Rohartgi, P. K. Indian J Textile Res 1986, 11, 86.
10. Yang, G. C.; Zeng, H. M.; Zhang, W. B. Cellulose Sci Technol 1995, 13, 15.
11. Yang, G. C.; Zeng, H. M.; Li, J. J.; Jian, N. B.; Zhang, W. B. Cellulose Sci Technol 1996, 35, 53.
12. Joseph, K.; Thomas, S.; Pavitrhan, C. Polymer 1996, 37, 5139.
13. Herrera-Franco, P. J.; Vlader-Gonzalez, A. Compos Part A: Appl Sci Manufact 2004, 35, 339.
14. Joseph, K.; Thomas, S.; Pavithran, C. J Appl Polym Sci 1993, 47, 1731.
15. Kalaprasad, G.; Joseph, K.; Thomas, S. J Mater Sci 1997, 32, 4261.
16. Mokoena, M. A.; Djokovic, V.; Luyt, A. S. J Mater Sci 2004, 39, 1.
17. Sapieha, S.; Allard, P.; Zang, Y. H. J Appl Polym Sci 1990, 41 2039.
18. Kalaprasad, G.; Francis, B.; Thomas, S.; Kumar, C. R.; Pavithran, C.; Groeninckx, G.; Thomas, S. Polym Int 2004, 53, 1624.